Title

Utilization of a magnetic field-driven microscopic motion for piezoelectric energy harvesting.

Journal

Nanoscale, 11(43)

ISSN

2040-3364

Authors

Kim, Sanggon

Ico, Gerardo

Bai, Yaocai

et al.

Publication Date

2019-11-01

DOI

10.1039/c9nr04722k

Peer reviewed

Utilization of magnetic field-driven microscopic motion for piezoelectric energy harvesting

Sanggon Kim[1,2,4], Gerardo Ico[1], Yaocai Bai[3], Steve Yang[4], Jung-Ho Lee[5], Yadong Yin[3,4], Nosang V. Myung[2,4*], and Jin Nam[1,4*].

Addresses:

[1]*Department of Bioengineering, University of California, Riverside, California 92521, United States*

[2]*Department of Chemical and Environmental Engineering, University of California, Riverside, California 92521, United States*

[3]*Department of Chemistry, University of California, Riverside, California 92521, United States*

[4]*Program of Materials Science and Engineering, University of California, Riverside, California 92521, United States*

[5]*Department of Materials Science and Chemical Engineering, Hanyang University, Ansan, Korea*

*Corresponding authors: jnam@engr.ucr.edu and myung@engr.ucr.edu

Abstract

In spite of recent advances in the development of high performing piezoelectric materials, their applications are typically limited to the direct conversion of mechanical impact energy to electrical energy, potentially risking mechanical failures. In this study, we developed piezoelectric poly(vinylidenefluoride-trifluoroethylene) (P(VDF-TrFE)) nanofibers integrated with SiO_2-shelled Fe_3O_4 magnetic nanoparticles, to utilize magnetic energy to reliably drive the piezoelectric effect. Specifically, we show that the shape of the magnetic nanoparticle exerts a significant effect on the efficiency of the magno-mechano-electrical energy conversion as magnetic nanorods exhibit approximately 70% enhancement in the electric field generation under cyclic magnetic fields as compared to nanospheres. Under an alternating magnetic field of 200 mT, the magnetic nanorod-piezoelectric nanofiber composite generated a peak-to-peak voltage of approximately 30 mV_{p-p} with a superior durability without any performance degradation after over 1 million cycles. This study demonstrates the potential of magnetic-field responsive, piezoelectric-based materials in the energy harvesting applications from non-mechanical energy sources.

Keywords: Piezoelectric electrospun nanofiber, Magnetic nanoparticle, Waste energy harvesting

Introduction

Energy demand for portable electronic devices has substantially increased due to the incorporation of power-guzzling features such as powerful computational capability, various sensors and larger screen size. To accommodate such a high energy demand, scavenging wasted energy sourced from daily-life activities has been explored with diverse approaches for efficient energy conversion. One of the most common and effective approaches is the conversion of mechanical energy to electrical energy. The mechanical energy mainly originates from human body or machine motions, and its energy output is considerably high among the other energy scavenging sources such as light, radio-frequency electromagnetic radiation, and thermal gradient.[1, 2] Therefore, piezoelectric materials, capable of converting mechanical energy to electrical energy, are the key to efficiently harvest such wasted energy.[3, 4]

For low frequency, high strain applications, polymer-based piezoelectric materials have significant advantages over piezo-ceramics due to their flexibility and impact resistance.[5] Among various polymeric piezoelectric materials, poly(vinylidene fluoride) (PVDF) has shown to exhibit outstanding piezoelectric constants[6] and fairly good thermal stability. Recently, the copolymerization of a phase stabilizer, trifluoride ethylene (TrFE), enables the maintenance of electrically active β-phase at room temperature, achieving greater piezoelectric constants.[4] We have further demonstrated that electrospinning process induces P(VDF-TrFE) nanofibers to form greater β-phase content without additional mechanical stretching and/or electric poling for piezo-ceramic compatible performances.[7, 8]

To further improve its utilization, the addition of functional materials, i.e., magnetic materials in the PVDF matrix, may enable to exploit other extrinsic stimuli, i.e. magnetic fields, to actuate the piezoelectric polymer for energy generation. Indeed, several groups have attempted

to introduce Fe_3O_4 nanoparticles into PVDF films[9] and nanofibers[10], and demonstrated that the addition of the nanoparticle enhances the piezoelectric performance due to an increase in β-phase formation and electret doping effect[11]. A few studies have reported to utilize magnetic fields to actuate piezoelectric devices at macroscale in combination with an additional magnetic materials[12, 13]. However, to the best of our knowledge, no report has yet demonstrated the magneto-mechano-electrical energy conversion at nanoscale by utilizing microscopic movement of the magnetic nanoparticles embedded within individual piezoelectric nanofibers, enabling a long-term structural stability. In this study, we developed a composite of P(VDF-TrFE) and Fe_3O_4 encapsulated by SiO_2, and demonstrated its performance in producing electric fields under alternating magnetic fields via the microscopic movement of magnetic nanoparticles, embedded in the piezoelectric nanofibers. Specifically, the effects of the morphological anisotropy of the magnetic nanoparticles on the piezoelectric performance of piezoelectric-magnetic composites were investigated to enhance the energy conversion.

Results and discussion

In this study, we aimed to develop an electrospun piezoelectric P(VDF-TrFE) composite with magnetic nanoparticles (MNPs) and demonstrate the actuation of the piezoelectric nanofibers by the microscopic movements of the MNPs under magnetic fields for electric field generation (Figure 1a). We particularly focused on examining the effects of MNP shape factor on the efficiency of magneto-mechano-electrical conversion. The mechanism underlying the conversion of magnetic field to mechanical strain to electrical energy is based on the microscopic movement of the MNPs straining P(VDF-TrFE) nanofibers due to two major forces: attractive force and

torque. The attractive force ($\boldsymbol{F_{att}}$) occurs when the MNPs are placed in a magnetic field gradient, causing convectional movements, which can be described by the equation,

$$\boldsymbol{F_{att}} = \nabla(\boldsymbol{m} \cdot \boldsymbol{B}) = \nabla \boldsymbol{m}\mathbf{B}\cos\theta, \quad (1)$$

where **m** is magnetic dipole moments, **B** is magnetic field, and θ is angle between $\boldsymbol{m}$ and $\boldsymbol{B}$ vectors.

Another force that the MNP will experience in the magnetic field is torque,

$$\boldsymbol{\tau_{mag}} = \boldsymbol{m} \times \boldsymbol{B} = \boldsymbol{m}\boldsymbol{B}sin\theta, \quad (2)$$

where its magnitude becomes maximum at $\theta = 90°$ while the maximum of the attractive force is at $\theta = 0°$. The torque induced by the magnetic field causes the rotation of an MNP, further microscopically straining the nanofiber, in addition to the tensile straining by $\boldsymbol{F_{att}}$. Based on the equations (1 and 2), the total force applied to the nanofiber is determined by $\boldsymbol{m}$, $\boldsymbol{B}$, and the magnetization orientation of MNPs. Therefore, the uniform alignment of MNP orientation is the key to maximize the overall force generated under magnetic fields. In this regard, the shape of MNP is essential for its alignment when embedded within an electrospun nanofiber; the MNP with an anisotropic morphology, i.e., rod shape, will promote the alignment of MNP magnetization along the long axis of the fiber while that with the spherical shape will result in statistically random magnetization orientation.

To investigate the effects of the MNP shape factor with different aspect ratios on the torque strain generation to the nanofibers, numerical simulation using COMSOL Multiphysics was conducted. In this simulation, maximum possible torque strains induced by the rotation of MNPs were compared; the direction of the MNP dipoles is all aligned along the nanofiber axis regardless of the particle shape. Figure 1c shows that the strain increases almost linearly with the increase of the aspect ratio when the same magnitude of force was applied to the opposite sides of the MNP surfaces in the axis parallel to nanofibers as shown in Figure 1b. Based on this simulation result,

we synthesized magnetic nanoparticles with a rod shape (magnetic nanorod (MNR)) or a spherical shape (magnetic nanosphere (MNS)) as shown in Figure 2 to demonstrate the particle shape dependency of magnetic field-induced piezoelectric nanofiber strain and its consequent electric field generation. The average diameter and length of the MNRs are approximately 160 nm and 460 nm, respectively, with 40 nm SiO_2 layer, which was indispensable to form such a shape with high aspect ratio[14]. The average diameter of the MNSs was controlled to match that of the MNRs at approximately 168 nm with 30 nm SiO_2 layer. These MNPs were separately dispersed in P(VDF-TrFE) solution prior to being subjected to electrospinning. We have previously reported that the reduction of the nanofiber diameter results in the exponential enhancement of piezoelectric properties due to the enhanced β-phase formation and Young's modulus[15]. For the present study, nanofiber diameter is more significant factor in determining electric field generation as compared to typical direct mechanical force induced applications due to minute strains generated by the microscopic movements of MNPs. Therefore, the reduction of nanofiber diameter without significantly deteriorating MNP distribution within the nanofibers, is critical to enhance the piezoelectric performance by promoting the strain of individual fibers, and by improving piezoelectric coefficients through dimensional reduction. In this regard, the diameters of both MNR and MNS composite nanofibers were carefully controlled, minimized, and matched to compare the magneto-mechano-electrical energy conversion induced by the MNP-derived actuation on piezoelectric nanofibers under alternating magnetic fields. The SEM images of Fe_3O_4@SiO_2 MNS and MNR/PVDF-TrFE nanofiber composites show that MNPs are uniformly distributed along the individual nanofibers (Figure 2c-d). The average diameters of MNP-containing fibers were approximately 58 nm (MNR) and 63 nm (MNS), respectively. It should be noted that MNPs are not embedded in the center of the nanofibers. The height profiles of the AFM

images show that MNPs are surrounded with at least 20 ~ 30 nm thick-layer of P(VDF-TrFE) resulting in robust mechanical bonding between MNPs and nanofibers, stable under strains (Figure 2e-f). Indeed, we did not observe any mechanical failure of MNPs separated from the nanofiber matrix in the subsequent experiments.

The piezoelectric properties of the nanofibers were determined by piezo-response force microscopy (PFM) (Figure 3a-b). Piezoelectric properties were analyzed by monitoring the amplitude changes with respect to the applied electric bias and showed a relatively similar response from MNR- and MNS-containing nanofibers. The values of the d_{33} for MNR-nanofiber and MNS-nanofiber were 36 ± 7 and 40 ± 14 pm/V, respectively, with around 60 nm fiber diameter. It is expected that the difference in the electric outputs under the same strain due to the discrepancy in d_{33} between MNR and MNS will be within the range of 10%.

Shape-dependent magnetization was analyzed by magnetic hysteresis loops (MHLs) to compare the magnetic properties of the MNR and MNS in nanofiber in Figure 3c-d. Higher remanence to saturation magnetization ratio (M_r/M_s) and coercivity indicates an easy magnetization direction or preferential direction of the magnetic dipole of the magnetic materials. The MHLs were conducted in two magnetic field directions: in-plane ($H//$) and out-of-plane ($H\perp$). Asymmetric shape of MNRs makes them aligned along the nanofiber axis during electrospinning. In the MHLs under $H\perp$, the angle between MNRs and H_a is 90 °. The parallel MHLs of MNR show higher M_r/M_s and H_c than perpendicular MHLs elucidating that the easy magnetization direction of the NR is the long axis of the NR (Figure 3c). Contrary to the MNRs, the polarity of the MNS is randomly oriented in the nanofibers due to its spherically symmetry structure. As expected from the structure, MHLs of MNS show that magnetic isotropy between the in-plane and out-of-plane field orientation, resulting in almost the same M_r/M_s and H_c (Figure

3d). The identical curves regardless of the direction of the applied magnetic fields elucidate that there is no preferential orientation of the MNS in the nanofiber mat (Figure 3f). These results confirm the superiority of MNR to maximize force generated under magnetic fields as described earlier (Figure 1). The amount of torqueing by MNPs under magnetic fields can be estimated by the MHL. The total mechanical work by the torque for the cyclic integral $\tau d\theta = -dW$ is proportional to the area of M-H loop.[16, 17] When comparing the area (A) of perpendicular MHLs of MNR and MNS, which represents the actual operating scheme of the experiment (perpendicular approach of the magnet to the surface of nanofiber mats), the ratio of A_{MNR}/A_{MNS} is approximately 1.4. Given the ratio, it is expected that 1.4 times larger torsional work is induced by the MNRs during the approach of the external magnet.

To confirm the superior piezoelectric performance of MNR-nanofiber expected from the piezoelectrical and magnetic characterization, electric outputs from the MNS and MNR composite nanofibers with a similar thickness of approximately 25 μm were measured under the cyclic movement of the magnet as shown in Figure 4a. The movement of the magnet was limited to the perpendicular direction to the nanofiber mat, thereby minimizing the contribution from electro-magnetic interference (EMI) on the electric output. The control experiment with P(VDF-TrFE) nanofibers without any MNPs confirmed that the influence of EMI is negligible (Figure 4b). Au-coated glass substrates were used as electrodes, sandwiching the samples to prevent macro-scale deformation of the nanofiber mat during the measurement. Representative electric outputs from MNR and MNS were plotted to compare their amplitude difference in Figure 4b. To validate the reproducibility, five independent nanofiber mats with either MNRs or MNSs were independently prepared and the electric outputs of each device were measured (Figure S1). The resultant electric outputs from MNR were an average of 30 mV_{p-p}, approximately 70 % higher than that of MNS at

an average of 21 mV_{p-p}. The electric outputs from as-spun PVDF-TrFE nanofiber showed negligible voltages, confirming that the generated voltages from MNP-containing fibers originates from the strain induced by the movement of the MNPs in the nanofibers. The output voltage with switching-polarity test further confirms that the signals were generated by the piezoelectric response of the devices (Figure S2). This electric output difference is above the level of 40% enhancement predicted from the magnetization area comparison in MHLs (Figure 3c-d), likely due to the combination of slightly higher piezoelectric constant, enhanced torqueing and different distribution of MNRs within the nanofiber matrix.

The electric outputs (voltage and current) of the current system under magnetic fields are considerably lower than that generated under direct mechanical actuation (Figure S3). However, this energy harvesting strategy has a significant advantage by providing a means to produce electrical energy without a macro-scale mechanical actuation that typically leads to mechanical failure and/or poor electrical contact after a long period usage. To demonstrate its long-term durability, the system was subjected to over 1 million cycles and showed a consistent electric output without any degradation as shown in Figure 4c. We expect that the electric output can be further improved by optimizing the load of the MNPs or the mat thickness.

Conclusion

In this work, we investigated MNPs with different morphologies embedded within piezoelectric P(VDF-TrFE) nanofibers for the magneto-mechano-electrical energy conversion. MNRs aligned along the nanofiber by the electrospinning process, which resulted in their uniform magnetization orientation in the direction of the long axis of MNR, enabling a full utilization of torque strain to enhance electric field generation under cyclic magnetic fields. The combination of enhancements

in the out-of-plane magnetization, the torque-induced strain generation, and the piezoelectric constant resulted in the enhanced energy conversion performance of the MNRs, generating 70% greater electric outputs as compared to MNS. These results demonstrate the significant impact of the particle shape factor on the MNP-based energy harvesting. Furthermore, the result from the durability test demonstrates that the microscopic movement of the nanofibers without macro-scale bending or compression enables long-term energy harvesting capability without degradation of piezoelectric performance over 1 million cycles. Therefore, this work opens another revenue as a waste energy harvesting strategy using a piezo electric polymer combined with magnetic nanoparticles.

Experimental

Synthesis of magnetic Fe_3O_4@SiO_2 nanorods (NRs)

The synthesis of FeOOH NRs was based on a previously reported methods[14, 18] with some modifications. In a typical synthesis of 460 nm FeOOH NRs, 100 mL of 0.1 M $FeCl_3$ aqueous solution was added into a glass vial, which was tightly sealed and kept at 87 °C for 24 h. After cooling to room temperature, the particles were collected by centrifugation, washed with water for several times, and dispersed in 20 mL of water. The surface of as-synthesized FeOOH NRs were functionalized with polyacrylic acid (PAA). To 20 mL of the above FeOOH dispersions, 20 mL of PAA solution (7.2 mg/mL) was added. The mixture was then stirred for 12 h, followed by centrifugation to remove excess PAA and re-dispersing in 20 mL of water. A 20 ml aqueous dispersion of PAA-modified FeOOH NRs was added into 100 mL of ethanol, followed by the addition of 3 mL of ammonium hydroxide (~28 % wt) and 4 mL of tetraethyl orthosilicate. After 4 h of reaction, the FeOOH@SiO_2 NRs were isolated by centrifugation, washed with ethanol and

water for several times, and dried at 60 °C. The FeOOH@SiO_2 NRs was reduced at 360 °C by 5% H_2 for 2 h to produce the Fe_3O_4@SiO_2 NRs.

Synthesis of magnetic Fe_3O_4@SiO_2 nanospheres (NSs)

Similar synthetic protocols were employed for the preparation of Fe_3O_4@SiO_2 NSs. In a typical synthesis, 100 mL of mixed aqueous solution of 0.2 M $FeCl_3$ and 0.08 M cetyltrimethylammonium chloride was tightly sealed in a glass bottle and kept at 87 °C for 24 h. The FeOOH NSs were then collected and washed, functionalized with PAA, coated with silica, and finally converted to Fe_3O_4@SiO_2 NSs by using the same protocols as for Fe_3O_4@SiO_2 NRs.

Electrospinning of MNP composite P(VDF-TrFE) nanofibers

0.36g of P(VDF-TrFE) (70/30 mol%, Solvay Group, France) was dissolved in 2.13g of N,N-dimethylformamide (DMF) (Fisher Scientific, Pittsburgh, PA) and 1.19g of acetone, supplemented with 0.31g of pyridinium formate (PF) buffer (Sigma-Aldrich, St Louis, MO) to increase the solution conductivity. After complete dissolution of P(VDF-TrFE) under magnetic stirring, 0.252 g of MNPs were added to the solution and sonicated for 1 hour. The solution was then elecrospun for 4 hours at applied voltage of ~15 kV with the distance of 20 cm between the needle and substrate at around 20 °C and a relative humidity of 9 g m^{-3}. The deposited electrospun nanofibers were then placed in an oven at 90 °C for 24 hours.

Numerical simulations

Solid mechanics module in COMSOL Multiphysics 5.3a was used for the numerical simulation (Figure 1b-c). The diameter of MNR and MNS was set at 160 nm. Nanofibers of 60 nm in diameter

and 4 μm in length were used, and their Young's modulus, Poisson's ratio, and density of the nanofiber were set at 50 GPa[15], 0.39, and 1780kg/m^3 [19], respectively. To calculate the torque strain induced by the rotation of MNPs, the same magnitude of force (1μN) was applied to the opposite sides of the MNP surfaces in the axis parallel to nanofibers. The average of the first principle strain in nanofibers was calculated with respect to the aspect ratio of the MNPs.

Characterization of MNP composite P(VDF-TrFE) nanofibers

The morphology of MNPs and MNP composite P(VDF-TrFE) nanofibers were characterized using transmission electron microscope (TEM, Tecnai 12) and scanning electron microsocope (SEM, FEI NNS450). MFP-3D AFM (Asylum Research, Santa Barbara, CA) was used for topographic images and piezoelectric coefficient measurement. The topographic images were obtained under tapping imaging mode, and the probe was then placed on the top of the individual fiber in contact mode subsequently by switching AFM to PFM mode. Under our PFM measurement system, single point spectroscopy was measured on the nanofibers on Au substrate and step voltages from -3 to +3 V were applied to the fiber and the amplitude change of the PFM cantilever (AC240TM, Olympus) was recorded in the same direction to the electric field which corresponds to the piezoelectric constant, d_{33}. Taking into account the quality factor (Q) of the AFM cantilever, the d_{33} of the nanofibers was calculated using the following relation,

$$d_{33} = \frac{A}{VQ} f \quad (3)$$

where A is the amplitude of the piezoresponse, V is the applied bias, and f is the correctional factor (*f=23.96)* from the periodically poled lithium niobite (PPLN) standard[20] which has a known piezoelectric coefficient. Room temperature magnetic hysteresis loops of the MNR and MNS in nanofiber were conducted with a vibrating sample magnetometer (DMS). Because the NR and NS

are integrated with the nanofiber mats with the same weight % and their thicknesses are similar (~25 μm), nanofiber mat area was based instead of mass for the direct comparison of the MNR and MNS in nanofiber. Hence, 1.5 cm by 1.5 cm nanofiber mats were cut into 9 small pieces (5 mm by 5 mm). The 9 small pieces of nanofibers were stacked and placed in the center of the magnetic hysteresis. The fibers were placed in two direction: in-plane (H//) and out-of-plane (H ⊥) and the external magnetic field was applied to the film at 10 Oe increment and 3s dwell time.

Electric output measurement under magnetic stimulus

100 nm Au was deposited on the both sides of the nanofiber mats (Area: 2.25 cm^2, Thickness: 25 μm) by sputtering and the samples were sandwiched with Au coated glasses for efficient collection of the generated charges from the nanofibers. A cube Neodymium magnet (N42 1-1/2") was used for the stimulus of the MNP-nanofiber mat. The magnetic field intensity measured using a gauss meter (HT20, Resolution: 1mT) on the surface of the south pole was ~ 200mT. To minimize electromagnetic interference and induced current due to the magnet, the magnet moved vertically to the fiber mat and the fiber was completely sealed with grounded aluminum (Al) film. The generated voltage was measured with an oscilloscope (Pico Technology, St Neots, United Kingdom) under the magnetic stimulation by a vertical cyclic movement of the magnet at 3.3Hz.

Conflicts of interest

There are no conflicts to declare.

Acknowledgement

This work was supported by the Creative Materials Discovery Program through the National Research Foundation of Korea funded by the Ministry of Science and ICT (2018M3D1A1057844), and UC Riverside and Korea Institute of Materials Science (Research Program POC2930) through UC-KIMS Center for Innovative Materials for Energy and Environment.

References

1. P. D. Mitcheson, E. M. Yeatman, G. K. Rao, A. S. Holmes and T. C. Green, *Proceedings of the IEEE*, 2008, **96**, 1457-1486.
2. J. Paulo and P. Gaspar, 2010.
3. S. Priya and D. J. Inman, *Energy harvesting technologies*, Springer, 2009.
4. C. Wan and C. R. Bowen, *Journal of Materials Chemistry A*, 2017, **5**, 3091-3128.
5. C. Wong, in *Polymers for Electronic & Photonic Application*, Elsevier, 1993, pp. 167-220.
6. Z. Pi, J. Zhang, C. Wen, Z.-b. Zhang and D. Wu, *Nano Energy*, 2014, **7**, 33-41.
7. M. Baniasadi, J. Huang, Z. Xu, S. Moreno, X. Yang, J. Chang, M. A. Quevedo-Lopez, M. Naraghi and M. Minary-Jolandan, *ACS applied materials & interfaces*, 2015, **7**, 5358-5366.
8. G. Ico, A. Myung, B. Kim, N. Myung and J. Nam, *Nanoscale*, 2018, **10**, 2894-2901.
9. A. S. Bhatt, D. K. Bhat and M. Santosh, *Journal of Applied Polymer Science*, 2011, **119**, 968-972.
10. A. Venugopal, O. Cespedes and S. Russell, *International Journal of Polymer Science*, 2014, **2014**.
11. J.-S. Im and I.-K. Park, *ACS applied materials & interfaces*, 2018, **10**, 25660-25665.
12. N. Cui, W. Wu, Y. Zhao, S. Bai, L. Meng, Y. Qin and Z. L. Wang, *Nano letters*, 2012, **12**, 3701-3705.
13. W.-H. Wu, K.-C. Kuo, Y.-H. Lin and Y.-C. Tsai, *Microelectronic Engineering*, 2018, **191**, 16-19.
14. M. Wang, L. He, W. Xu, X. Wang and Y. Yin, *Angewandte Chemie International Edition*, 2015, **54**, 7077-7081.
15. G. Ico, A. Showalter, W. Bosze, S. C. Gott, B. S. Kim, M. P. Rao, N. V. Myung and J. Nam, *Journal of Materials Chemistry A*, 2016, **4**, 2293-2304.
16. V. Vega, V. M. Prida, J. A. García and M. Vazquez, *physica status solidi (a)*, 2011, **208**, 553-558.
17. G. Bertotti and I. D. Mayergoyz, *The science of hysteresis: Hysteresis in materials*, Gulf Professional Publishing, 2006.
18. X. Wang, J. Feng, H. Yu, Y. Jin, A. Davidson, Z. Li and Y. Yin, *Research*, 2018, **2018**, 7527825.
19. H. Gallantree, *IEE Proceedings I-Solid-State and Electron Devices*, 1983, **130**, 219-224.
20. S. Xie, A. Gannepalli, Q. N. Chen, Y. Liu, Y. Zhou, R. Proksch and J. Li, *Nanoscale*, 2012, **4**, 408-413.

Figure Captions

Figure 1. Conversion of magnetic energy to electric energy by utilizing dynamic strains induced by microscopic movements of magnetic Fe_3O_4@SiO_2 nanorod (MNR)- and nanosphere (MNS)-composite P(VDF-TrFE) nanofibers under magnetic fields. (a) Schematic illustration of MNR and MNS embedded in P(VDF-TrFE) nanofibers under magnetic fields. (b) A schematic of nanofiber strain induced by the torque of the magnetic nanoparticles. (c) Average first principle strain in nanofibers due to the torque of the MNRs with different aspect ratio. Finite element analysis in COMSOL Multiphysics was used to obtain the simulation results of (b) and (c). The values are normalized to that of MNS (i.e., aspect ratio = 1).

Figure 2. Morphological characterization of magnetic nanoparticles (MNPs) and P(VDF-TrFE) nanofibers. TEM images of magnetic Fe_3O_4@SiO_2 (a) nanorods (MNRs) and (b) nanospheres (MNSs). SEM images of electrospun P(VDF-TrFE) nanofibers with (c) MNRs and (d) MNSs. AFM images of (e) MNR and (f) MNS embedded in P(VDF-TrFE) nanofibers. Insets show the cross-sectional topography of the fiber (A) with and (B) without MNPs.

Figure 3. Piezoelectric and magnetic characterization of electrospun P(VDF-TrFE) nanofibers embedded with magnetic Fe_3O_4@SiO_2 nanorods (MNRs) and nanospheres (MNSs). Piezoelectric responses of the nanofibers with (a) MNRs and (b) MNSs (top graphs) in response to applied electric biases (bottom graphs). In-plane ($H//$) and out-of-plane ($H\perp$) magnetic hysteresis loops of the nanofibers with (c) MNRs and (d) MNSs. Schematic illustration of magnetic nanoparticle polarization under $H//$ and $H\perp$ showing that (e) all MNRs are aligned in the direction of nanofibers and their magnetization orientation are also in the same direction with the nanofibers while (f) MNSs have randomly oriented magnetization.

Figure 4. Electric outputs of approximately 25 μm-thick electrospun mats composed of magnetic Fe_3O_4@SiO_2 nanoparticle embedded P(VDF-TrFE) nanofibers under magnetic stimulation by a vertical cyclic movement of a neodymium magnet. (a) Schematic of the device assembly to measure electric outputs under magnetic stimulation. (b) Comparison of electric outputs from as-

spun P(VDF-TrFE) nanofiber mat, its composite with MNSs, or MNR. (c) A long-term durability test of P(VDF-TrFE) nanofibers embedded with MNRs.

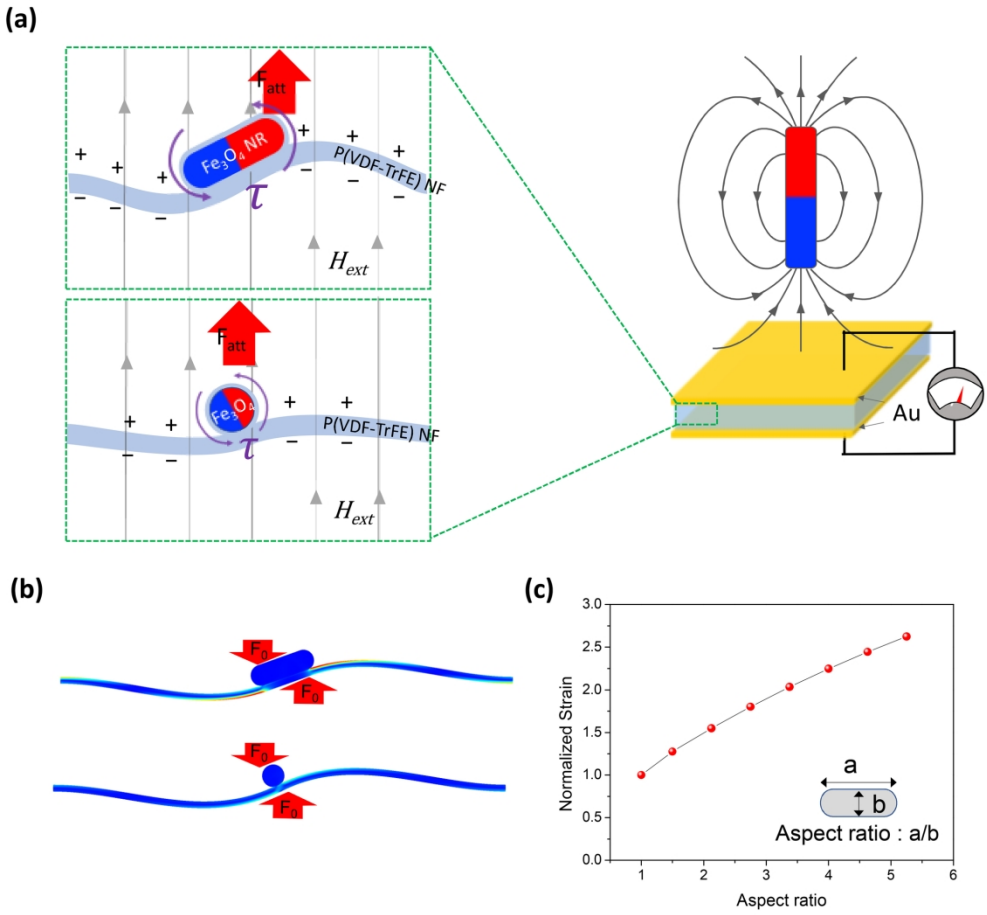

Figure 1. Conversion of magnetic energy to electric energy by utilizing dynamic strains induced by microscopic movements of magnetic Fe3O4@SiO2 nanorod (MNR)- and nanosphere (MNS)- composite P(VDF-TrFE) nanofibers under magnetic fields. (a) Schematic illustration of MNR and MNS embedded in P(VDF-TrFE) nanofibers under magnetic fields. (b) A schematic of nanofiber strain induced by the torque of the magnetic nanoparticles. (c) Average first principle strain in nanofibers due to the torque of the MNRs with different aspect ratio. Finite element analysis in COMSOL Multiphysics was used to obtain the simulation results of (b) and (c). The values are normalized to that of MNS (i.e., aspect ratio = 1).

190x177mm (300 x 300 DPI)

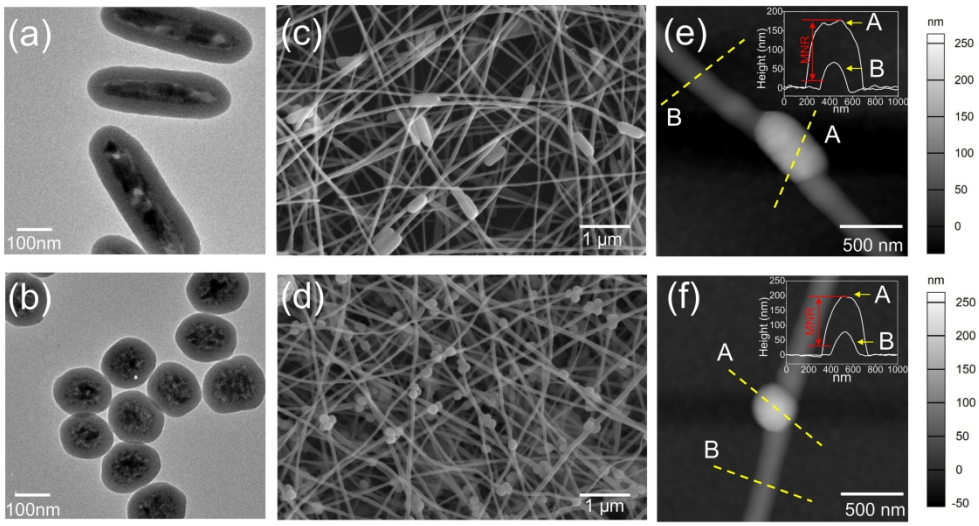

Figure 2. Morphological characterization of magnetic nanoparticles (MNPs) and P(VDF-TrFE) nanofibers. TEM images of magnetic Fe3O4@SiO2 (a) nanorods (MNRs) and (b) nanospheres (MNSs). SEM images of electrospun P(VDF-TrFE) nanofibers with (c) MNRs and (d) MNSs. AFM images of (e) MNR and (f) MNS embedded in P(VDF-TrFE) nanofibers. Insets show the cross-sectional topography of the fiber (A) with and (B) without MNPs.

215x114mm (300 x 300 DPI)

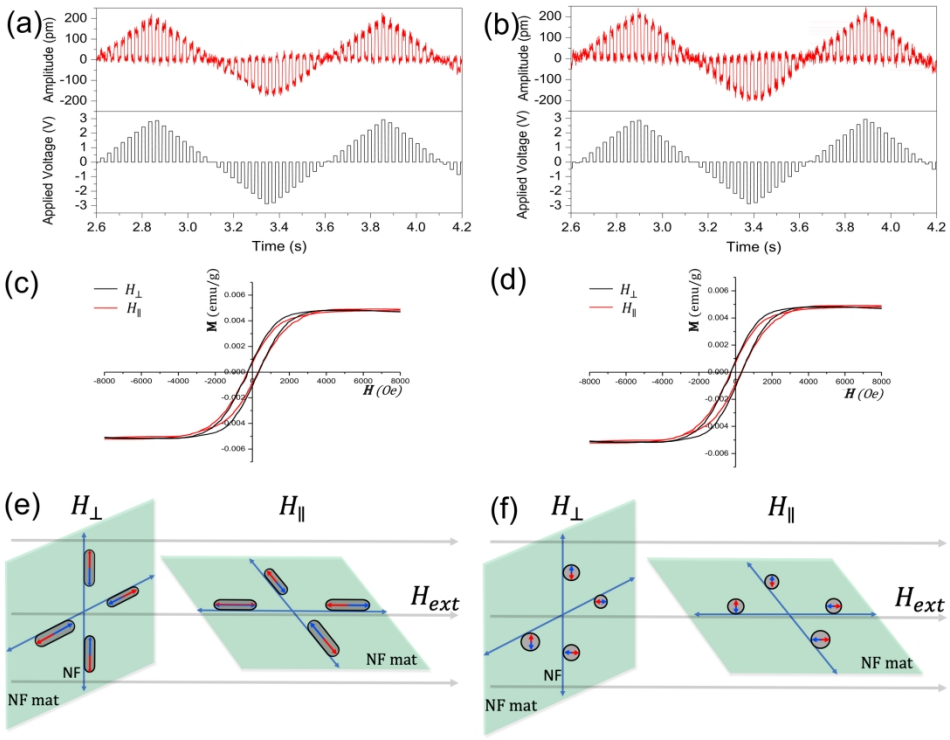

Figure 3. Piezoelectric and magnetic characterization of electrospun P(VDF-TrFE) nanofibers embedded with magnetic Fe3O4@SiO2 nanorods (MNRs) and nanospheres (MNSs). Piezoelectric responses of the nanofibers with (a) MNRs and (b) MNSs (top graphs) in response to applied electric biases (bottom graphs). In-plane (H//) and out-of-plane (H⊥) magnetic hysteresis loops of the nanofibers with (c) MNRs and (d) MNSs. Schematic illustration of magnetic nanoparticle polarization under H// and H⊥ showing that (e) all MNRs are aligned in the direction of nanofibers and their magnetization orientation are also in the same direction with the nanofibers while (f) MNSs have randomly oriented magnetization.

215x171mm (300 x 300 DPI)

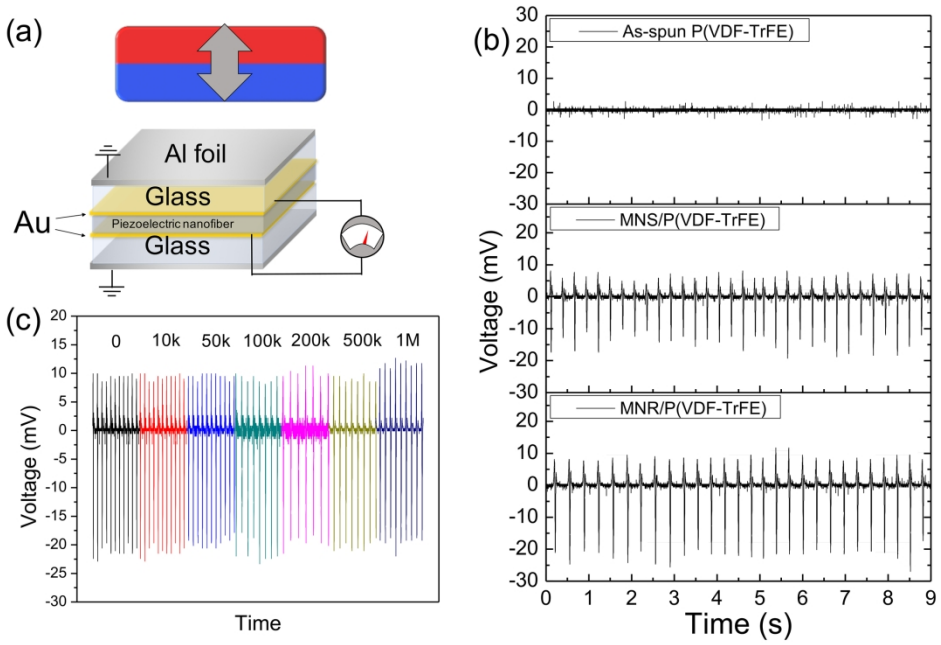

Figure 4. Electric outputs of approximately 25 μm-thick electrospun mats composed of magnetic Fe3O4@SiO2 nanoparticle embedded P(VDF-TrFE) nanofibers under magnetic stimulation by a vertical cyclic movement of a neodymium magnet. (a) Schematic of the device assembly to measure electric outputs under magnetic stimulation. (b) Comparison of electric outputs from as-spun P(VDF-TrFE) nanofiber mat, its composite with MNSs, or MNR. (c) A long-term durability test of P(VDF-TrFE) nanofibers embedded with MNRs.

215x156mm (300 x 300 DPI)

Table of Contents

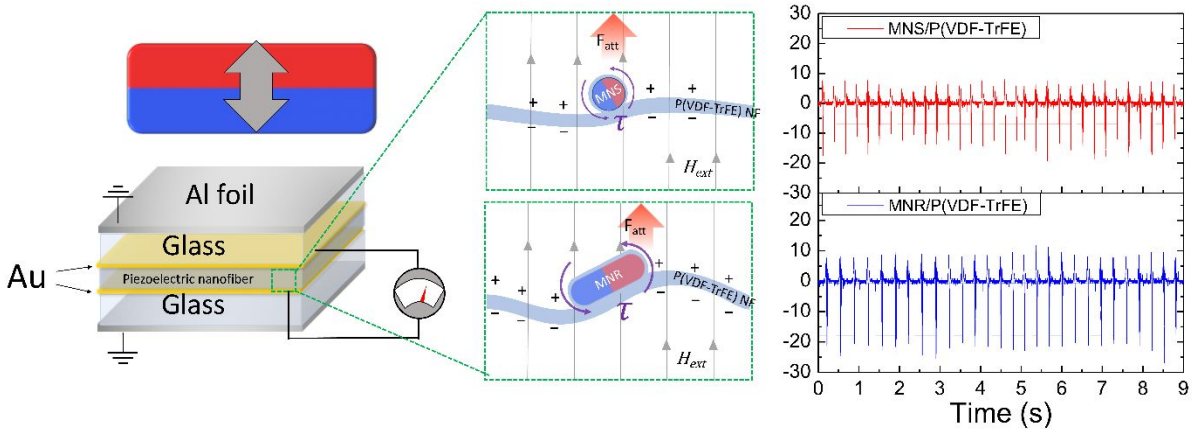

Magneto-mechano-electrical energy conversion in poly(vinylidenefluoride-trifluoroethylene) piezoelectric nanofibers integrated with magnetic nanoparticles in a particle-shape dependent manner

Supporting information

Utilization of magnetic field-driven microscopic motion for piezoelectric energy harvesting

Sanggon Kim[1,2,4], Gerardo Ico[1], Yaocai Bai[3], Steve Yang[4], Jung-Ho Lee[5], Yadong Yin[3,4], Nosang V. Myung[2,4*], and Jin Nam[1,4*].

Addresses:

[1]*Department of Bioengineering, University of California, Riverside, California 92521, United States*

[2]*Department of Chemical and Environmental Engineering, University of California, Riverside, California 92521, United States*

[3]*Department of Chemistry, University of California, Riverside, California 92521, United States*

[4]*Program of Materials Science and Engineering, University of California, Riverside, California 92521, United States*

[5]*Department of Materials Science and Chemical Engineering, Hanyang University, Ansan, Korea*

*Corresponding authors: jnam@engr.ucr.edu and myung@engr.ucr.edu

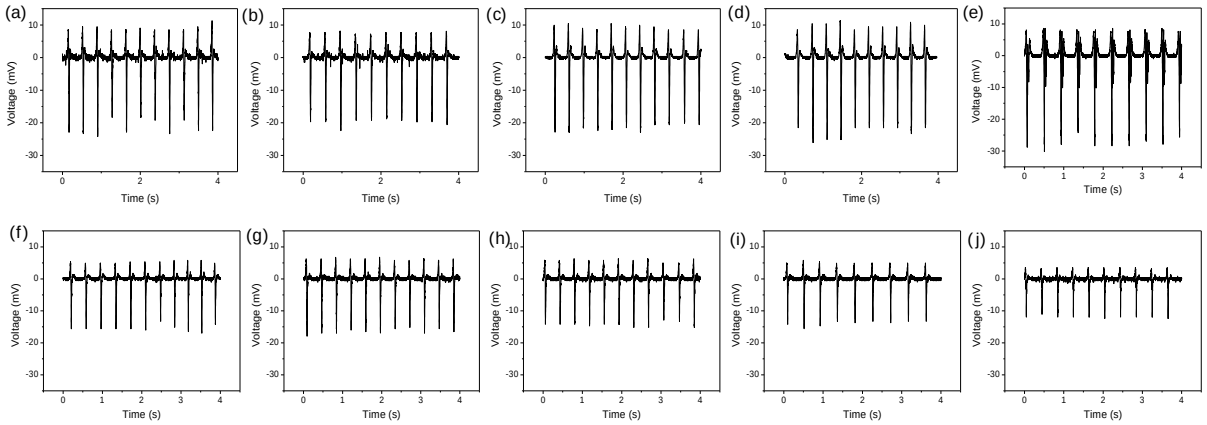

Figure S1. Reproducibility test of the piezoelectric output voltage measured from five independent P(VDF-TrFE) nanofiber mats with MNRs (a-e) and MNSs (f-j).

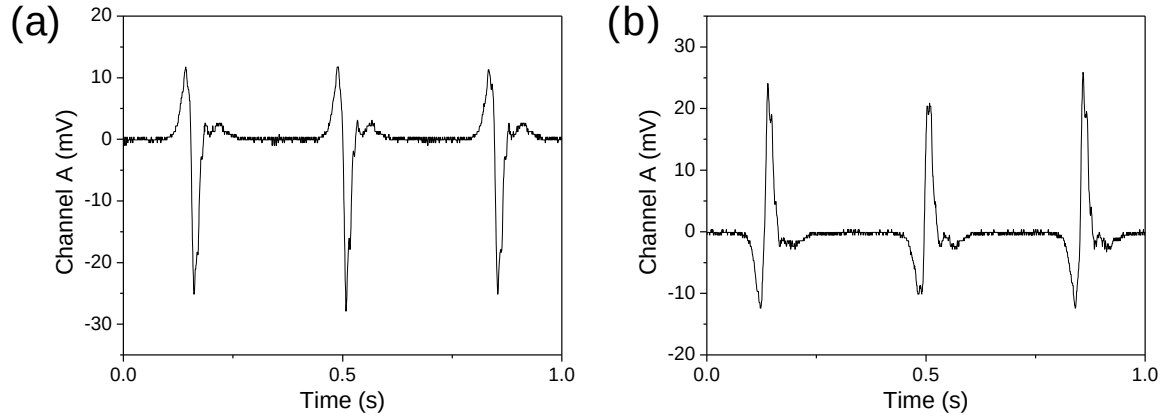

Figure S2. Piezoelectric output voltage measured from the magnetic Fe_3O_4@SiO_2 nanorodes embedded P(VDF-TrFE) nanofiber mats by (a) forward and (b) reverse connections.

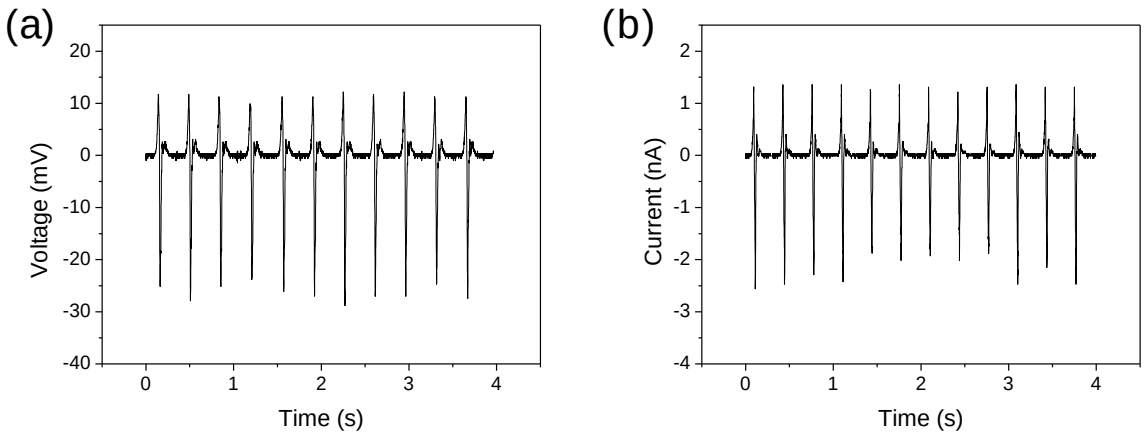

Figure S3. Piezoelectric (a) open-circuit voltage and (b) short-circuit current measured from the magnetic Fe_3O_4@SiO_2 nanorodes embedded P(VDF-TrFE) nanofiber mats.